

ExoMol molecular line lists V: The ro-vibrational spectra of NaCl and KCl

Emma J. Barton¹, Christopher Chiu¹, Shirin Golpayegani¹, Sergei N. Yurchenko¹, Jonathan Tennyson¹, Daniel J. Frohman² and Peter F. Bernath²

¹*Department of Physics and Astronomy, University College London, London WC1E 6BT, UK;*

²*Department of Chemistry and Biochemistry, Old Dominion University, Norfolk 23529-0126, USA*

Accepted XXXX. Received XXXX; in original form XXXX

ABSTRACT

Accurate rotation-vibration line lists for two molecules, NaCl and KCl, in their ground electronic states are presented. These line lists are suitable for temperatures relevant to exoplanetary atmospheres and cool stars (up to 3000 K). Isotopologues $^{23}\text{Na}^{35}\text{Cl}$, $^{23}\text{Na}^{37}\text{Cl}$, $^{39}\text{K}^{35}\text{Cl}$, $^{39}\text{K}^{37}\text{Cl}$, $^{41}\text{K}^{35}\text{Cl}$ and $^{41}\text{K}^{37}\text{Cl}$ are considered. Laboratory data was used to refine *ab initio* potential energy curves in order to compute accurate ro-vibrational energy levels. Einstein A coefficients are generated using newly determined *ab initio* dipole moment curves calculated using the CCSD(T) method. New Dunham Y_{ij} constants for KCl are generated by a reanalysis of a published Fourier transform infrared emission spectra. Partition functions plus full line lists of ro-vibration transitions are made available in an electronic form as supplementary data to this article and at www.exomol.com.

molecular data; opacity; astronomical data bases: miscellaneous; planets and satellites: atmospheres; stars: low-mass

1 INTRODUCTION

NaCl and KCl are important astrophysical species as they are simple, stable molecules containing atoms of relatively high cosmic abundance. Na, K and Cl are the 15th, 20th and 19th most abundant elements in the interstellar medium (Caris et al. 2004). In fact NaCl could be as abundant as the widely-observed SiO molecule (Cernicharo & Guelin 1987). Cernicharo & Guelin (1987) reported the first detection of metal halides, NaCl, KCl, AlCl and, more tentatively, AlF, in the circumstellar envelope of carbon star IRC+10216. These observations have been followed up recently by Agundez et al. (2012), who also observed CS, SiO, SiS and NaCN. NaCl has also been detected in the circumstellar envelopes of oxygen stars IK Tauri and VY Caris Majoris (Milam et al. 2007). Another environment in which these molecules have been found is the tenuous atmosphere of Jupiter’s moon Io. Submillimetre lines of NaCl, and more tentatively KCl, were detected by Lellouch et al. (2003) and Moullet et al. (2013) respectively. NaCl has also been identified in the cryovolcanic plumes of Saturn’s moon Enceladus alongside its constituents Na and Cl (Postberg et al. 2011). K was also detected but the presence of KCl could not be confirmed. Furthermore NaCl and KCl are expected to be present in Super Earth atmospheres (Schaefer et al. 2012) and may form in the observable atmosphere of the known object GJ1214b (Kreidberg et al. 2014).

The alkali chlorides are also of industrial importance as they are products of coal and straw combustion. Their presence in coal increases the rate of corrosion in coal fired power plants (Yang et al. 2014). Therefore it is important to monitor their concentrations, which can be done spectroscopically provided the appropriate data is available.

The importance of NaCl and KCl spectra have motivated a number of laboratory studies, for example Rice & Klemperer (1957); Honig et al. (1954); Horiai et al. (1988); Uehara et al. (1989); Clouser & Gordy (1964); Uehara et al. (1990). The most recent and extensive research on KCl and NaCl spectra has been performed by Ram et al. (1997), whom investigated infrared emission lines of Na^{35}Cl , Na^{37}Cl and $^{39}\text{K}^{35}\text{Cl}$, Caris et al. (2004), whom measured microwave and millimetre wave lines of $^{39}\text{K}^{35}\text{Cl}$, $^{39}\text{K}^{37}\text{Cl}$, $^{41}\text{K}^{35}\text{Cl}$, $^{41}\text{K}^{37}\text{Cl}$ and $^{40}\text{K}^{35}\text{Cl}$, and Caris et al. (2002), whom recorded microwave and millimetre wave lines of Na^{35}Cl and Na^{37}Cl .

Dipole moment measurements have been carried out by Leeuw et al. (1970) for Na^{35}Cl and Na^{37}Cl , Wachem & Dymanus (1967) for $^{39}\text{K}^{35}\text{Cl}$ and $^{39}\text{K}^{37}\text{Cl}$, and Hebert et al. (1968) for $^{39}\text{K}^{35}\text{Cl}$, Na^{35}Cl and Na^{37}Cl .

It appears the only theoretical transition line lists for these molecules are catalogued in the Cologne Database for Molecular Spectroscopy (CDMS), see Müller et al. (2005). They were constructed using data reported in Caris et al. (2002); Clouser & Gordy (1964); Uehara et al. (1989); Leeuw et al. (1970) for NaCl, and Caris et al. (2004); Clouser & Gordy (1964); Wachem & Dymanus (1967) for KCl. The lists are limited to $v = 4$, $J = 159$ and do not include a list for $^{41}\text{K}^{37}\text{Cl}$. In this paper we aim to compute more comprehensive line lists for the previously studied isotopologues and the first theoretical line list for $^{41}\text{K}^{37}\text{Cl}$.

The ExoMol project aims to provide line lists on all the molecular transitions of importance in the atmospheres of planets. The aims, scope and methodology of the project have been summarised by Tennyson & Yurchenko (2012). Lines lists for $\text{X } ^2\Sigma^+ \text{XH}$ molecules, $\text{X} = \text{Be, Mg, Ca}$, and $\text{X } ^1\Sigma^+ \text{SiO}$ have already been published (Yadin et al. (2012); Barton et al. (2013) respectively). In this paper, we present ro-vibrational transition lists and associated spectra for two NaCl and four KCl isotopologues.

2 METHOD

The nuclear motion Schrödinger equation allowing for Born-Oppenheimer Breakdown (BOB) affects, is solved for species XCl using program LEVEL (Le Roy 2007). To initiate these calculations, program DPOTFIT (Le Roy 2006) was used to generate a refined potential energy curve (PEC) for each molecule by fitting *ab initio* curves to laboratory data.

2.1 Spectroscopic Data

The most comprehensive and accurate sets of available laboratory measurements are the infrared ro-vibrational emission lines of Ram et al. (1997) and the microwave rotational lines of Caris et al. (2002) and Caris et al. (2004) all of which were recorded at temperatures in the region of 1000 C, see Table 1. For KCl Fourier transform infrared emission spectra measured by Ram et al. (1997) has been re-analysed and re-assigned as part of this work, see Section 2.2. The Dunham constants (Y_{ij}) obtained from this new fit are provided in Table 2. Ro-vibrational emission lines derived from this were used in place of those presented by Ram et al. (1997) because of problems found in the previous analysis.

2.2 Reanalysis of the KCl infrared spectrum

Ram et al. (1997) reported spectroscopic constants derived from an infrared emission spectrum of KCl recorded with a high resolution Fourier transform spectrometer (FTS). By using the new constants derived from the millimetre wave spectrum by Caris et al. (2004) to simulate the infrared spectrum of $^{39}\text{K}^{35}\text{Cl}$ with PGOPHER (Western 2013), it was clear that Ram et al. (1997) had mis-assigned much of the complex spectrum. The Ram et al. (1997) spectrum was therefore re-analyzed. As a first step, the millimetre wave line list from Caris et al. (2004) was refitted with the addition of two Dunham parameters, Y_{23} and Y_{41} . These parameters were found to improve the quality of the fit. The Caris et al. (2004) constants plus Y_{23} and Y_{41} were then used to calculate band constants used as input for PGOPHER. Using PGOPHER the infrared line positions were selected manually and then refitted along with the Caris data using our LSQ fit program. There were 253 R branch lines of $^{39}\text{K}^{35}\text{Cl}$ fit from the 6-5, 5-4, 4-3, 3-2, 2-1, and 1-0 bands, and the Y_{10} , Y_{20} and Y_{30} vibrational constants were added. The quality of the observed spectrum was insufficient to fit additional bands or P branch lines. The final constants from our global fit are compared to the values reported by Caris et al. (2004) in Table 2. The Y_{10} and Y_{20} (ω_e and $-\omega_e x_e$) constants of Caris et al. (2004) were derived entirely from millimetre wave data using Dunham relationships and are in good agreement with the values we have determined directly from infrared observations.

2.3 Dipole Moments

Experimental measurements of the permanent dipole as a function of vibrational state have been performed by Leeuw et al. (1970); Wachem & Dymanus (1967); Hebert et al. (1968) who considered NaCl, KCl and both molecules respectively. Additionally Pluta (2001) calculated dipole moments at equilibrium bond length as part of theoretical study comparing various levels of theory (SCF, MP2, CCSD and CCSD(T)). Giese & York (2004) computed NaCl dipole moment curves (DMCs) using a multi-reference configuration interaction (MRCI) approach and extrapolated basis sets. However there appears to be no published KCl dipole moment curves (DMCs), experimental or *ab initio*.

We determined new DMCs for both molecules using high-level *ab initio* calculations, shown in Fig. 1. These were performed using MOLPRO (Werner et al. 2010). The final NaCl DMC was computed using an aug-cc-pCVQZ-DK basis set and the CCSD(T) method, where the both core-valence and relativistic effects were also taken into account. Inclusion of both effects is known to be important (Tennyson 2014). In case of KCl, an effective core potential ECP10MDF (MCDHF+Breit) in conjunction with the corresponding basis set (Lim et al. 2005) was used for K and aug-cc-pV(Q+d)Z was used for Cl. In

Table 1. Summary of laboratory data used to refine the KCl and NaCl potential energy curves. Temperatures are those given in the cited papers. Uncertainties are the maximum quoted uncertainty given in the cited papers.

Reference	Transitions	Frequency range (cm ⁻¹)	Uncertainty (cm ⁻¹)
Caris et al. (2002)	$\Delta v = 0, \Delta J = \pm 1$ Na ³⁵ Cl, $v = 0 - 5, J \leq 72$ Na ³⁷ Cl, $v = 0 - 4, J \leq 76$	6.6 – 31	6.7×10^{-6}
Caris et al. (2004)	$\Delta v = 0, \Delta J = \pm 1$ ³⁹ K ³⁵ Cl, $v = 0 - 7, J \leq 127$ ³⁹ K ³⁷ Cl, $v = 0 - 7, J \leq 129$ ⁴¹ K ³⁵ Cl, $v = 0 - 6, J \leq 128$ ⁴¹ K ⁴⁷ Cl, $v = 0 - 5, J \leq 131$	5.6 – 31	6.7×10^{-6}
Ram et al. (1997)	$\Delta v = 1, \Delta J = \pm 1$ Na ³⁵ Cl, $v = 0 - 8, J \leq 118$ Na ³⁹ Cl, $v = 0 - 3, J \leq 91$	240 – 390	0.005
This work	$\Delta v = 1, \Delta J = +1$ ³⁹ K ³⁵ Cl, $v = 0 - 6, J \leq 131$	240 – 390	0.005

Table 2. Dunham Constants (in cm⁻¹) of the X ¹Σ⁺ state of KCl. (Uncertainties are given in paranthesis in units of the last digit.)

Constant	This Work	Caris et al. (2004)
Y ₀₁	0.1286345842(27)	0.1286345835(38)
Y ₁₁	-7.896827(31)E-4	-7.896870(24)E-4
Y ₂₁	1.5916(14)E-6	1.59637(59)E-6
Y ₃₁	5.47(27)E-9	4.297(50)E-9
Y ₄₁	-7.6(18)E-11	-
Y ₀₂	-1.0868336(42)E-7	-1.0868276(72)E-7
Y ₁₂	-1.112(19)E-11	-1.184(13)E-11
Y ₂₂	3.729(30)E-12	3.851(15)E-12
Y ₀₃	-2.0955(35)E-14	-2.0975(64)E-14
Y ₁₃	3.614(65)E-16	3.877(37)E-16
Y ₂₃	4.4(10)E-18	-
Y ₀₄	-4.019(99)E-20	-4.04(19)E-20
Y ₁₀	279.88193(76)	279.889346(936)
Y ₂₀	-1.19671(26)	-1.1972502(793)
Y ₃₀	0.003094(26)	-

both cases the electric dipole moment were obtained using the finite field method. The *ab initio* DMC grid points were used directly in LEVEL. Equilibrium bond length dipole moments are compared in Table 3. Our computed equilibrium dipole for KCl is about 1 % larger than the experimental value. For NaCl this difference is closer to 2 % but our final, CCSD(T) value is close to those calculated by Giese & York (2004).

2.4 Fitting the Potentials

The *ab initio* PECs were refined by fitting to the spectroscopic data identified in Table 1. However, extending the temperature range of the spectra requires consideration of highly excited levels and extrapolation of the PECs beyond the region determined by experimental input values, hence care needs to be taken to ensure the curves maintain physical shapes outside

Table 3. Comparison of Na³⁵Cl and ³⁹K³⁵Cl dipole moments at equilibrium internuclear distance.

Reference	Method	μ (NaCl) Debye	μ (KCl) Debye
Hebert et al. (1968)	Experiment	8.9721	10.2384
Pluta (2001)	SCF	9.2774	10.6626
Pluta (2001)	MP2	9.0740	10.4923
Pluta (2001)	CCSD	9.0715	10.4847
Pluta (2001)	CCSD(T)	9.0257	10.4542
This work	CCSD(T)	9.1430	10.3119

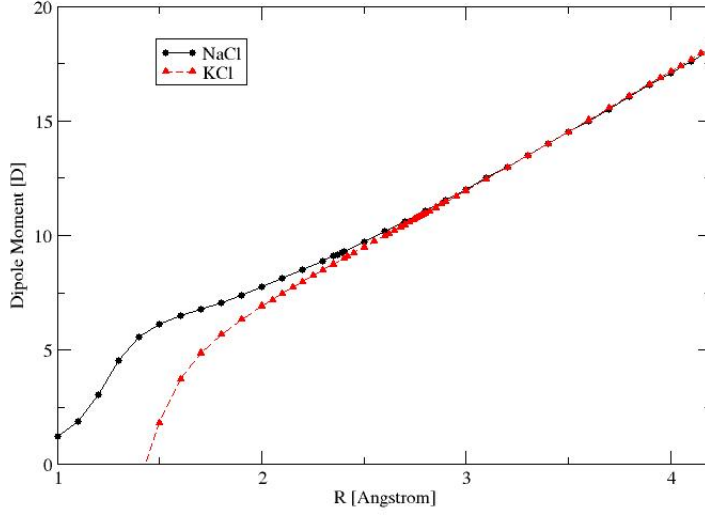


Figure 1. *Ab initio* dipole moment curves for NaCl and KCl in their ground electronic states.

the experimentally refined regions. In this context we define a physical shape to be the shape of the *ab initio* curve. We tested multiple potential energy forms, namely the extended Morse oscillator (EMO), Morse long range (MLR) and Morse Lenard Jones (MLJ) potentials Le Roy (2011), to achieve an optimum fit to the experimental data whilst maintaining a physical curve shape. Data for multiple isotopologues were fitted simultaneously to ensure the resulting curves are valid for all isotopologues. r_e and D_e were held constant in the fits, as the fits were found to be unstable otherwise.

For NaCl, BOB terms did not improve the quality of the fit and were not pursued. Of the 1370 lines used in the fit, 1060 were Na^{35}Cl and 310 were Na^{37}Cl . The final potential was expressed as an EMO:

$$V(r) = D_e \left[1 - e^{-\phi(r)(r-r_e)} \right]^2, \quad (1)$$

where

$$\phi(r) = \sum_{i=0}^N \phi_i y_p(r, r_e)^i, \quad (2)$$

$$y_p(r, r_e) = \frac{r^p - r_e^p}{r^p + r_e^p} \quad (3)$$

and p was set to 3, N to 4, D_e to 34120.0 cm^{-1} (Huber & Herzberg 1979), and r_e to 2.360796042 \AA (Ram et al. 1997). Parameters resulting from the fit are given in Table 4.

For KCl non-adiabatic BOB terms were included in the fit as they resulted in an improvement. Of the 549 lines used in the fit, 361 were $^{39}\text{K}^{35}\text{Cl}$, 82 were $^{39}\text{K}^{37}\text{Cl}$, 64 were $^{41}\text{K}^{35}\text{Cl}$ and 40 were $^{41}\text{K}^{37}\text{Cl}$. The final potential was expressed as a MLR:

$$V(r) = D_e \left[1 - \frac{u_{\text{LR}}(r)}{u_{\text{LR}}(r_e)} e^{-\phi(r)(r-r_e)} \right]^2, \quad (4)$$

where

$$\phi(r) = \sum_{i=0}^N \phi_i y_p(r, r_e)^i + y_p(r, r_e) \phi_\infty, \quad (5)$$

$$y_p(r, r_e) = \frac{r^p - r_e^p}{r^p + r_e^p} \quad (6)$$

$$u_{\text{LR}}(r) = \frac{C_m}{r^m} + \frac{C_n}{r^n} \quad (7)$$

Table 4. Fitting parameters used in the NaCl Extended Morse Oscillator potential, see eq. (1). (Uncertainties are given in parenthesis in units of the last digit.)

N	ϕ_i
0	0.8947078(17)
1	-0.287528(48)
2	0.00581(11)
3	-0.0278(14)
4	-0.0290(37)

Table 5. Fitting parameters used in the KCl Morse Long Range potential, see eq. (4). (Uncertainties are given in parenthesis in units of the last digit.)

N	ϕ_i	t_j
0	-9.075210(10)	0.0
1	1.23590(85)	0.00030(12)
2	0.4859(22)	0.0
3	1.200(10)	0.0

and p was set to 2, N to 3, m to 2, n to 3, C_2 to 10000, C_3 to 13000000, D_e to 34843.15 cm⁻¹ (Brewer & Brackett 1961) and r_e to 2.6667253989 Å (Caris et al. 2004).

The non-adiabatic BOB correction function is defined as:

$$g(r) = \frac{M^{ref}}{M} \left[y_p(r, r_e) t_\infty + [1 - y_p(r, r_e)] \sum_{j=0}^N t_j [y_p(r, r_e)]^j \right] \quad (8)$$

where

$$y_p(r, r_e) = \frac{r^p - r_e^p}{r^p + r_e^p} \quad (9)$$

and M is the mass of the particular isotopologue, M_{ref} is the mass of the parent isotopologue, p was set to 2 and N to 1. Parameters resulting from this fit are given in Table 5.

The input experimental data was reproduced within 0.01 cm⁻¹ and often much better than this. The final curves, shown in Fig 2, follow the *ab initio* shape with the exception of regions 6Å – 17Å for KCl and 4.5Å – 8Å for NaCl. These regions are associated with the textbook avoided crossings between Columbic X⁺ – Cl⁻ and neutral X – Cl PECs which occurs in the adiabatic representation of the ground electronic state, see Giese & York (2004) for a detailed discussion. Without experimental data near dissociation it is difficult to represent this accurately with DPOTFIT. Consequently we decided to limit our line lists to vibrational states lying below 20,000 cm⁻¹ which do not sample these regions. This has consequences for the temperature range considered. Based on our partition sum, see Section 2.5, this range is 0 – 3000 K.

Comparisons with observed frequencies for Na³⁵Cl and ³⁹K³⁵Cl are given in Table 6 and 7. These demonstrate the accuracy of fits. An important aim in refining a PEC is to also predict spectroscopic data outside the experimental range. This can be tested for KCl for which there are R band head measurements up to $v = 12$ (Ram et al. 1997). The positions of

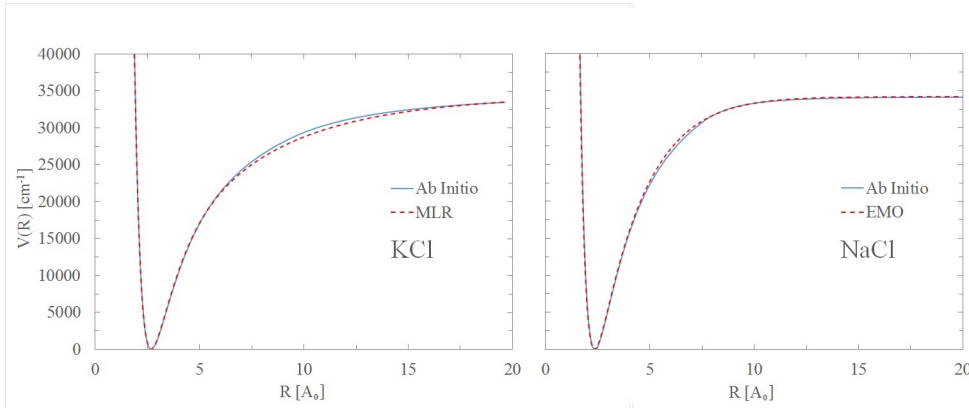
**Figure 2.** Comparison of *ab initio* and fitted ground electronic state potential energy curves for NaCl (left) and KCl (right).

Table 6. Comparison of theoretically predicted Na³⁵Cl ro-vibrational wavenumbers, in cm⁻¹, with some of the laboratory measurements of Ram et al. (1997).

v'	J'	v''	J''	Obs.	Calc.	Obs.-Calc.
1	99	0	98	387.0444	387.0446	-0.0002
1	100	0	99	387.1219	387.1221	-0.0002
1	101	0	100	387.1950	387.1957	-0.0007
2	3	1	2	358.9248	358.9260	-0.0012
2	4	1	3	359.3419	359.3444	-0.0025
2	5	1	4	359.7587	359.7596	-0.0009
3	110	2	109	380.2722	380.2746	-0.0024
3	111	2	110	380.3014	380.3075	-0.0061
3	112	2	111	380.3372	380.3365	0.0007
4	28	3	27	361.3425	361.3429	-0.0004
4	29	3	28	361.6718	361.6730	-0.0012
4	31	3	30	362.3244	362.3230	0.0014
5	3	4	2	348.6060	348.6104	-0.0044
5	4	4	3	349.0193	349.0195	-0.0002
5	5	4	4	349.4289	349.4254	0.0035
6	114	5	113	369.5373	369.5406	-0.0033
6	115	5	114	369.5551	369.5562	-0.0011
6	117	5	116	369.5781	369.5758	0.0023
7	73	6	72	362.1649	362.1606	0.0043
7	74	6	73	362.3244	362.3276	-0.0032
7	75	6	74	362.4924	362.4910	0.0014
8	38	7	37	350.7058	350.7009	0.0049
8	39	7	38	350.9881	350.9876	0.0005
8	40	7	39	351.2687	351.2710	-0.0023

these band heads, which are key features in any weak or low-resolution spectrum, are predicted to high accuracy, see Table 8.

2.5 Partition Functions

The calculated energy levels, see Section 3, were summed in Excel to generate partition function values for a range of temperatures. We determined that our partition function is at least 95% converged at 3000 K and much better than this at lower temperatures. Therefore temperatures up to 3000 K were considered. Values for the parent isotopologues are compared to previous studies, namely Irwin (1981), Sauval & Tatum (1984) and CDMS, in Table 9.

For ease of use, we fitted our partition functions, Q , to a series expansion of the form used by Vidler & Tennyson (2000):

$$\log_{10} Q(T) = \sum_{n=0}^6 a_n [\log_{10} T]^n \quad (10)$$

with the values given in Table 10.

2.6 Line-List Calculations

While sodium has only a single stable isotope, ²³Na, both potassium and chlorine each have two: ³⁹K (whose natural terrestrial abundance is about 93.25%) and ⁴¹K (6.73%), and ³⁵Cl (75.76%) and ³⁷Cl (24.24%). Line lists were therefore calculated for two NaCl and four KCl isotopologues. Ro-vibrational states up to $v = 100$, $J = 563$ and $v = 120$, $J = 500$ respectively, and all transitions between these states satisfying the dipole selection rule $\Delta J = \pm 1$, were considered. A summary of each line list is given in Table 11.

The procedure described above was used to produce line lists, i.e. catalogues of transition frequencies ν_{ij} and Einstein coefficients A_{ij} for two NaCl and four KCl isotopologues: Na³⁵Cl, Na³⁷Cl, ³⁹K³⁵Cl, ³⁹K³⁷Cl, ⁴¹K³⁵Cl and ⁴¹K³⁷Cl. The computed line lists are available in electronic form as supplementary information to this article.

3 RESULTS

The full line list computed for all isotopologue considered is summarised in Table 11. Each line list contains around 4 – 7 million transitions and are therefore, for compactness and ease of use, divided into separate energy files and transition files.

Table 7. Comparison of theoretically predicted $^{39}\text{K}^{35}\text{Cl}$ ro-vibrational wavenumbers, in cm^{-1} , with some of the laboratory data of Ram et al. (1997), as re-assigned in this work.

v'	J'	v''	J''	Obs.	Calc.	Obs.-Calc.
1	102	0	101	294.9349	294.9347	0.0002
1	103	0	102	295.0173	295.0154	0.0019
1	104	0	103	295.0955	295.0941	0.0014
1	105	0	104	295.1729	295.1710	0.0019
2	43	1	42	284.5787	284.5795	-0.0008
2	49	1	48	285.6588	285.6551	0.0037
2	51	1	50	286.0004	286.0001	0.0003
2	52	1	51	286.1646	286.1700	-0.0054
3	121	2	120	291.1544	291.1554	-0.0010
3	122	2	121	291.2013	291.1992	0.0021
3	123	2	122	291.2433	291.2411	0.0022
3	126	2	125	291.3562	291.3555	0.0007
4	74	3	73	284.6069	284.6019	0.0050
4	75	3	74	284.7309	284.7300	0.0009
4	76	3	75	284.8579	284.8563	0.0016
4	78	3	77	285.1054	285.1036	0.0018
5	111	4	110	285.7192	285.7174	0.0018
5	113	4	112	285.8341	285.8375	-0.0034
5	114	4	113	285.8912	285.8947	-0.0035
5	116	4	115	286.0004	286.0037	-0.0033
6	73	5	72	279.6821	279.6817	0.0004
6	75	5	74	279.9388	279.9355	0.0033
6	76	5	75	280.0552	280.0598	-0.0047
6	81	5	80	280.6586	280.6552	0.0034

Table 8. Comparison of theoretically predicted $^{39}\text{K}^{35}\text{Cl}$ R-branch band heads, in cm^{-1} , with laboratory measurements from Ram et al. (1997) and this work.

Band	Observed	Calculated	O – C
1 – 0	296.702	296.703	-0.001
2 – 1	294.181	294.182	-0.001
3 – 2	291.680	291.682	-0.002
4 – 3	289.201	289.203	-0.002
5 – 4	286.742	286.745	-0.003
6 – 5	284.303	284.306	-0.003
7 – 6	281.884	281.887	-0.003
8 – 7	279.488	279.489	-0.001
9 – 8	277.110	277.110	0.0
10 – 9	274.752	274.752	0.0
11 – 10	272.414	272.411	0.003
12 – 11	270.120	270.090	0.03

This is done using the standard ExoMol format (Tennyson et al. 2013) which is based on a method originally developed for the BT2 line list (Barber et al. 2006). Extracts from the start of the Na^{35}Cl and $^{39}\text{K}^{35}\text{Cl}$ files are given in Table 12, Table 14, Table 13 and Table 15. They can be downloaded from the CDS via XXX. The line lists and partition functions can also be obtained from www.exomol.com.

Figure 3 illustrates the synthetic absorption spectra of Na^{35}Cl and $^{39}\text{K}^{35}\text{Cl}$ at 300 K. As the dipole moment curves are essentially straight lines, the overtone bands for these molecules are very weak meaning that key spectral features are confined to long wavelengths associated with the pure rotational spectrum and the vibrational fundamental.

The CDMS database contains 607 and 772 rotational lines for Na^{35}Cl and $^{39}\text{K}^{35}\text{Cl}$ respectively. Comparisons with the CDMS lines are presented in Figure 4. As can be seen the agreement is excellent for both frequency and intensity. In particular, predicted line intensities agree within 2% and 4% for the KCl and NaCl isotopomers considered in CDMS respectively.

Emission cross-sections for Na^{35}Cl and $^{39}\text{K}^{35}\text{Cl}$ were simulated using Gaussian line-shape profiles with half-width = 0.01 cm^{-1} as described by Hill et al. (2013). The resulting synthetic emission spectra are compared to the experimental ones in Figs. 5 and 6. When making comparisons one has to be aware of a number of experimental issues. The baseline in NaCl shows residual "channeling": a sine-like baseline that often appears in FTS spectra due to interference from reflections from parallel

Table 9. Comparison of Na³⁵Cl and ³⁹K³⁵Cl partition functions

T(K)	This work	CDMS	Irwin (1981)	Sauval & Tatum (1984)
Na ³⁵ Cl				
9.375	30.3338	30.3307	-	-
18.75	60.3352	60.3299	-	-
37.5	120.3556	120.3455	-	-
75	240.6984	240.6770	-	-
150	496.6455	496.5538	-	-
225	802.3712	802.1167	-	-
300	1173.0397	1172.5403	-	-
500	2506.9232	2505.0340	-	-
1000	8161.702	-	8204.6	8165.4
1500	17333.48	-	17409.8	16960.3
2000	30294.77	-	30370.1	29685.3
2500	47362.31	-	47324.9	46807.2
3000	68909.60	-	68530.1	68766.1
³⁹ K ³⁵ Cl				
9.375	51.1529	51.1495	-	-
18.75	101.9823	101.9724	-	-
37.5	203.6737	203.6504	-	-
75	409.1563	409.1053	-	-
150	876.2078	876.0902	-	-
225	1474.9611	1474.7618	-	-
300	2225.1732	2224.8905	-	-
500	5000.7402	5000.3352	-	-
1000	17092.48	-	17277.73	17112.5
1500	36808.46	-	37327.7	36147.1
2000	64110.97	-	65747.4	64142.9
2500	99023.43	-	103058.6	102212.0
3000	142068.17	-	149837.7	151368.0

Table 10. Fitting parameters used to fit the partition functions, see eq. 10. Fits are valid for temperatures between 500 and 3000 K.

	Na ³⁵ Cl	Na ³⁷ Cl	³⁹ K ³⁵ Cl	³⁹ K ³⁷ Cl	⁴¹ K ³⁵ Cl	⁴¹ K ³⁷ Cl
a_0	35.528812	39.941335	372.555818	72.206029	74.926932	72.591531
a_1	-65.142353	-73.36368	-762.782356	-138.3407430	-143.689312	-139.093018
a_2	53.290409	59.6576584	653.21703	114.10145500	118.474798	114.705511
a_3	-23.592248	-26.212185	-297.787108	-50.41476400	-52.319838	-50.665015
a_4	6.036705	6.64133762	76.294719	12.68394200	13.1500522	12.740842
a_5	-0.8370958	-0.9113382	-10.405679	-1.71634070	-1.7770609	-1.7230912
a_6	0.04887272	0.05266306	0.5898907	0.097426548	0.1007164997	0.0977526634

optical surfaces in the beam. For KCl the spectrum is very weak and the baseline, which has a large offset, was not properly adjusted to zero. Given these considerations, the comparisons must be regarded as satisfactory.

4 CONCLUSIONS

We present accurate but comprehensive line lists for the stable isotopologues of NaCl and KCl. Laboratory frequencies are reproduced to much more than sub-wavenumber accuracy. This accuracy should extend to all predicted transition frequencies up to at least $v = 8$ and $v = 12$ for NaCl and KCl respectively. New *ab initio* dipole moments and Einstein A coefficients are computed. Comparisons with the semi-empirical CDMS database suggest the intensities the pure rotational are accurate.

Table 11. Summary of our line lists.

	Na ³⁵ Cl	Na ³⁷ Cl	³⁹ K ³⁵ Cl	³⁹ K ³⁷ Cl	⁴¹ K ³⁵ Cl	⁴¹ K ³⁷ Cl
Maximum v	100	100	120	120	120	120
Maximum J	557	563	500	500	500	500
Number of lines	4734567	4763324	7224331	7224331	7224331	7224331

Table 12. Extract from start of states file for Na³⁵Cl

I	\tilde{E}	g	J	v
1	0.000000	16	0	0
2	0.434501	48	1	0
3	1.303497	80	2	0
4	2.606971	112	3	0
5	4.344901	144	4	0
6	6.517259	176	5	0

I : State counting number; \tilde{E} : State energy in cm⁻¹; g : State degeneracy; J : State rotational quantum number; v : State vibrational quantum number.

Table 13. Extract from start of states file for ³⁹K³⁵Cl

I	\tilde{E}	g	J	v
1	0.0	16	0	0
2	0.256466	48	1	0
3	0.769393	80	2	0
4	1.538778	112	3	0
5	2.564613	144	4	0
6	3.846887	176	5	0

I : State counting number; \tilde{E} : State energy in cm⁻¹; g : State degeneracy; J : State rotational quantum number; v : State vibrational quantum number.

Table 14. Extracts from the transitions file for Na³⁵Cl

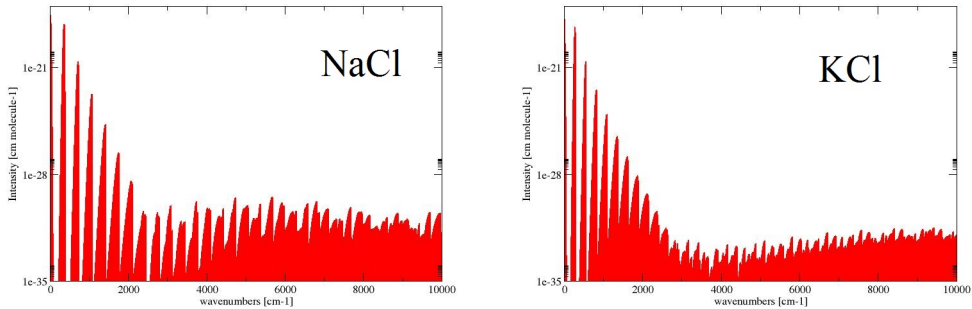
I	F	A_{IF}
2	1	7.21E-07
3	2	6.93E-06
4	3	2.50E-05
5	4	6.16E-05
6	5	1.23E-04
7	6	2.16E-04

I : Upper state counting number; F : Lower state counting number; A_{IF} : Einstein A coefficient in s⁻¹.

Table 15. Extracts from the transitions file for ³⁹K³⁵Cl

I	F	A_{IF}
2	1	1.89E-07
3	2	1.81E-06
4	3	6.55E-06
5	4	1.61E-05
6	5	3.21E-05
7	6	5.64E-05

I : Upper state counting number; F : Lower state counting number; A_{IF} : Einstein A coefficient in s⁻¹.


Figure 3. Absorption spectra of Na³⁵Cl and ³⁹K³⁵Cl at 300 K.

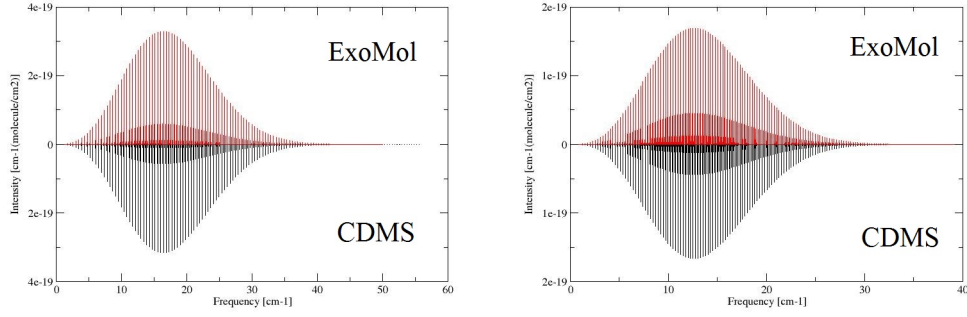


Figure 4. Absorption lines of Na^{35}Cl and $^{39}\text{K}^{35}\text{Cl}$ at 300 K: ExoMol vs. CDMS.

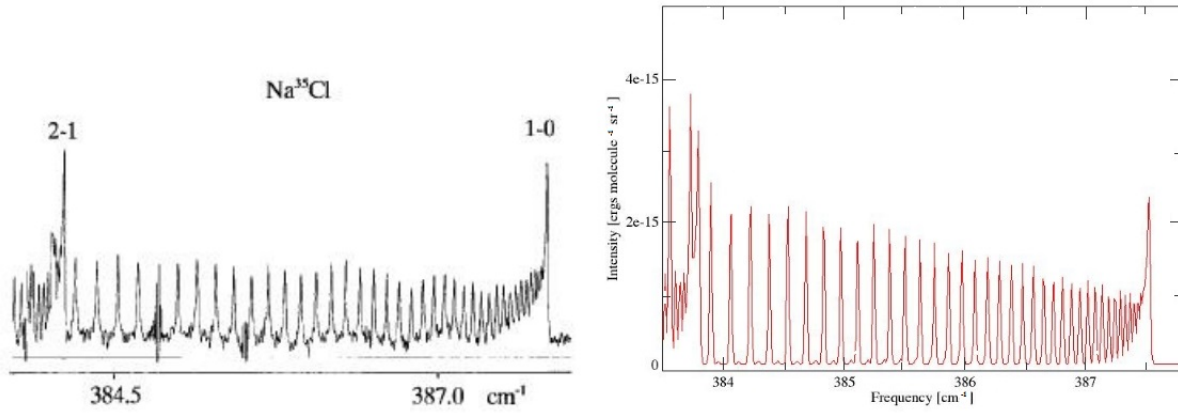


Figure 5. Emission spectra of NaCl at 1273 K: left, Ram et al. (1997); right, ExoMol. (Reprinted from Ref. (Ram et al. 1997). Copyright 1997, with permission from Elsevier.)

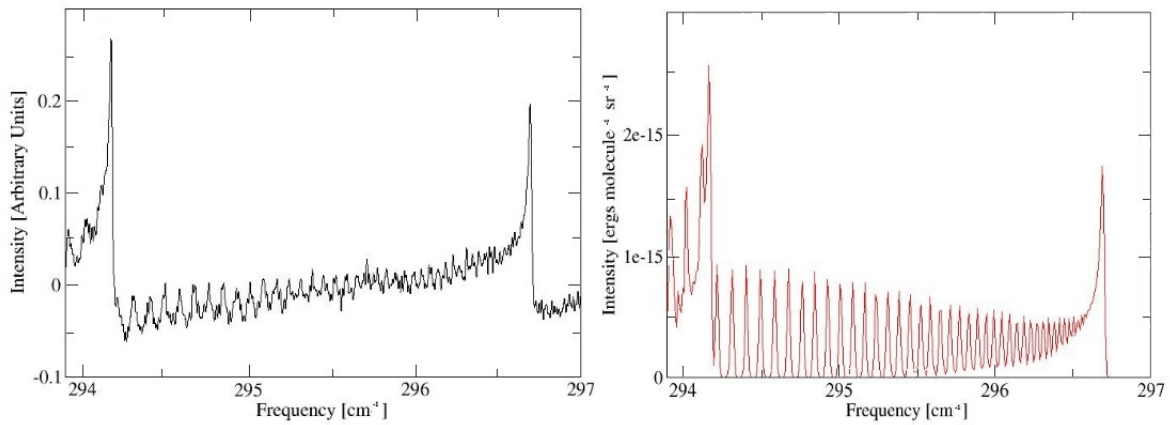


Figure 6. Emission spectra of KCl at 1273 K: left, Ram et al. (1997); right, ExoMol.

The results are line lists for the rotation-vibration transitions within the ground states of Na³⁵Cl, Na³⁷Cl, ³⁹K³⁵Cl, ³⁹K³⁷Cl, ⁴¹K³⁵Cl and ⁴¹K³⁷Cl, which should be accurate for a range of temperatures up to at least 3000 K. The line lists can be downloaded from the CDS or from www.exomol.com.

Finally, we note that HCl is likely to be the other main chlorine-bearing species in exoplanets. A comprehensive line lists for H³⁵Cl and H³⁷Cl have recently been provided by Li et al. (2013a) and Li et al. (2013b).

ACKNOWLEDGEMENTS

We thank Alexander Fateev for stimulating discussions and Kevin Kindley for some preliminary work with the KCl infrared emission spectrum. This work was supported by grant from energinet.dk under a subcontract from the Danish Technical University and by the ERC under the Advanced Investigator Project 267219. Support was also provided by the NASA Origins of Solar Systems program.

REFERENCES

- Agundez M., Fonfria J. P., Cernicharo J., Kahane C., Daniel F., Guelin M., 2012, *A&A*, 543, A48
- Barber R. J., Tennyson J., Harris G. J., Tolchenov R. N., 2006, *MNRAS*, 368, 1087
- Barton E. J., Yurchenko S. N., Tennyson J., 2013, *MNRAS*, 434, 1469–1475
- Brewer L., Brackett E., 1961, *Chem. Rev.*, 61, 425
- Caris A., Lewen F., Muller H. S. P., Winnewisser G., 2004, *J. Molec. Struct. (THEOCHEM)*, 695, 243
- Caris M., Lewen F., Winnewisser G., 2002, *Z. Naturforsch. Sect. A-J. Phys. Sci.*, 57, 663
- Cernicharo J., Guelin M., 1987, *A&A*, 183, L10
- Clouser P. L., Gordy W., 1964, *Phys. Rev. A*, 134, 863
- Giese T. J., York D. M., 2004, *J. Chem. Phys.*, 120, 7939
- Hebert A. J., Lovas F. J., Melendres C. A., Hollowell C. D., Story Jr T. L., Street Jr K., 1968, *J. Chem. Phys.*, 48, 2824
- Hill C., Yurchenko S. N., Tennyson J., 2013, *Icarus*, 226, 1673
- Honig A., Mandel M., Stitch M. L., Townes C. H., 1954, *Phys. Rev.*, 96, 629
- Horiai K., Fujimoto T., Nakagawa K., Uehara H., 1988, *Chem. Phys. Lett.*, 147, 133
- Huber K. P., Herzberg G., 1979, *Molecular Spectra and Molecular Structure IV. Constants of Diatomic Molecules*. Van Nostrand Reinhold Company, New York
- Irwin A. W., 1981, *ApJS*, 45, 621
- Kreidberg L. et al., 2014, *Nature*, 505, 66
- Le Roy R., 2011, *Equilibrium Structures of Molecules*, Taylor and Francis, London, pp. 159–203
- Le Roy R. J., 2006, *DPotFit 1.1 A Computer Program for Fitting Diatomic Molecule Spectral Data to Potential Energy Functions*. University of Waterloo Chemical Physics Research Report CP-662R, <http://leroy.uwaterloo.ca/programs/>
- Le Roy R. J., 2007, *LEVEL 8.0 A Computer Program for Solving the Radial Schrödinger Equation for Bound and Quasibound Levels*. University of Waterloo Chemical Physics Research Report CP-663, <http://leroy.uwaterloo.ca/programs/>
- Leeuw F. H., Wachem R., Dymanus A., 1970, *J. Chem. Phys.*, 53, 981
- Lellouch E., Paubert G., Moses J. I., Schneider N. M., Strobel D. F., 2003, *Nature*, 421, 45
- Li G., Gordon I. E., Hajigeorgiou P. G., Coxon J. A., Rothman L. S., 2013a, *J. Quant. Spectrosc. Radiat. Transf.*, 130, 284
- Li G., Gordon I. E., Le Roy R. J., Hajigeorgiou P. G., Coxon J. A., Bernath P. F., Rothman L. S., 2013b, *J. Quant. Spectrosc. Radiat. Transf.*, 121, 78
- Lim I. S., Schwerdtfeger P., Metz B., Stoll H., 2005, *J. Chem. Phys.*, 122
- Milam S. N., Apponi A. J., Woolf N. J., Ziurys L. M., 2007, *ApJ*, 668, L131
- Moulet A., Lellouch E., Moreno R., Gurwell M., Black J. H., Butler B., 2013, *ApJ*, 776, 32
- Müller H. S. P., Schlöder F., Stutzki J., Winnewisser G., 2005, *J. Molec. Struct. (THEOCHEM)*, 742, 215
- Pluta T., 2001, *Mol. Phys.*, 99, 1535
- Postberg F., Schmidt J., Hillier J., Kempf S., Srama R., 2011, *Nature*, 474, 620
- Ram R. S., Dulick M., Guo B., Zhang K. Q., Bernath P. F., 1997, *J. Mol. Spectrosc.*, 183, 360
- Rice S. A., Klemperer W., 1957, *J. Chem. Phys.*, 27, 573
- Sauval A. J., Tatum J. B., 1984, *ApJS*, 56, 193
- Schaefer L., Lodders K., Fegley B., 2012, *ApJ*, 755, 41
- Tennyson J., 2014, *J. Mol. Spectrosc.*, 296, 1
- Tennyson J., Hill C., Yurchenko S. N., 2013, in *AIP Conference Proceedings*, Vol. 1545, 6th international conference on atomic and molecular data and their applications ICAMDATA-2012, AIP, New York, pp. 186–195
- Tennyson J., Yurchenko S. N., 2012, *MNRAS*, 425, 21

- Uehara H., Horiai K., Konno T., Miura K., 1990, Chem. Phys. Lett., 169, 599
- Uehara H., Horiai K., Nakagawa K., Fujimoto T., 1989, J. Mol. Spectrosc., 134, 98
- Vidler M., Tennyson J., 2000, J. Chem. Phys., 113, 9766
- Wachem R., Dymanus A., 1967, J. Chem. Phys., 46, 3749
- Werner H. J., Knowles P. J., Lindh R., Manby F. R., Schütz M., 2010, MOLPRO, a package of ab initio programs. See <http://www.molpro.net/>
- Western C. M., 2013, PGOPHER 8.0, A program for simulating rotational structure. University of Bristol, <http://pgopher.chm.bris.ac.uk>
- Yadin B., Vaness T., Conti P., Hill C., Yurchenko S. N., Tennyson J., 2012, MNRAS, 425, 34
- Yang T., Kai X., Li R., Sun Y., He Y., 2014, Energy Souces A, 36, 15